

Monte Carlo–Type Neural Operator for Differential Equations

1st Salah Eddine Choutri

NYUAD Research Institute

New York University Abu Dhabi
Abu Dhabi, UAE

choutri@nyu.edu

2nd Prajwal Chauhan

Engineering Division

New York University Abu Dhabi
Abu Dhabi, UAE

pc3377@nyu.edu

3rd Othmane Mazhar

Laboratoire de Probabilités, Statistique et Modélisation

Sorbonne University & Université Paris Cité
Paris, France

omazhar@lpsm.paris

4th Saif Eddin Jabari

Engineering Division

New York University Abu Dhabi
Abu Dhabi, UAE

sej7@nyu.edu

Abstract—The Monte Carlo-type Neural Operator (MCNO) introduces a framework for learning solution operators of partial differential equations (PDEs) by directly learning the kernel function and approximating the associated integral operator using a Monte Carlo-type approach. Unlike Fourier Neural Operators (FNOs), which rely on spectral representations and assume translation-invariant kernels, MCNO makes no such assumptions. The kernel is represented as a learnable tensor over sampled input–output pairs, and sampling is performed once, uniformly at random from a discretized grid. This design enables generalization across multiple grid resolutions without relying on fixed global basis functions or repeated sampling during training, while an interpolation step maps between arbitrary input and output grids to further enhance flexibility. Experiments on standard 1D PDE benchmarks show that MCNO achieves competitive accuracy with efficient computational cost. We also provide a theoretical analysis proving that the Monte Carlo estimator yields a bounded bias and variance under mild regularity assumptions. This result holds in any spatial dimension, suggesting that MCNO may extend naturally beyond one-dimensional problems. More broadly, this work explores how Monte Carlo-type integration can be incorporated into neural operator frameworks for continuous-domain PDEs, providing a theoretically supported alternative to spectral methods (such as FNO) and to graph-based Monte Carlo approaches (such as the Graph Kernel Neural Operator, GNO).

Index Terms—Machine learning, Neural operator, Monte Carlo integration, Parametric PDEs, Theoretical bounds

I. INTRODUCTION

Neural networks have shown remarkable success in learning mappings between finite-dimensional vector spaces, particularly in image, language, and scientific modeling tasks. Extending this capability to mappings between infinite-dimensional function spaces has led to the development of neural operators, a class of models that approximate solution operators for partial differential equations (PDEs). These models aim to learn the operator that maps problem inputs, such as coefficients, boundary conditions, or forcing terms, to PDE solutions, enabling rapid inference after training and generalization across parameterized problem families.

One of the earliest operator learning architectures, the Deep Operator Network (DeepONet) [1], uses separate networks (branch and trunk) to learn nonlinear mappings from input functions to solution function evaluations. More recently, the Fourier Neural Operator (FNO) [2] introduced a spectral convolution approach, learning Fourier multipliers and leveraging the Fast Fourier Transform (FFT) to efficiently approximate the solution operator of a PDE via an integral formulation. FNO assumes the underlying integral kernel to be translation invariant and typically operates on uniform grids with periodic boundary conditions, making it efficient. However, it can struggle to represent localized or non-periodic phenomena [3].

To improve spatial localization and multi-scale modeling, wavelet-based neural operators have been proposed. The Multi-wavelet Transform Operator (MWT) [4] and the Wavelet Neural Operator (WNO) [5] apply compactly supported wavelets to enable hierarchical and localized operator learning. Another direction is the Convolutional Neural Operator (CNO) [6], which adapts convolutional networks to operator learning by applying spatial filters over structured grid data. This design enables local feature modeling and performs well on problems with regular grid discretizations.

A related approach is the Graph Neural Operator (GNO) [7], which extends operator learning to irregular spatial domains using graph message passing. GNO approximates the integral kernel through local aggregation across graph edges, resembling Monte Carlo integration in the graph setting. While it supports unstructured meshes, GNO has been evaluated on structured grids represented as regular graphs. In contrast, our suggested neural operator approximates the integral operator without relying on graph construction or repeated neighborhood aggregation, offering a simpler and more direct formulation.

In this work, we propose the Monte Carlo-type Neural Operator (MCNO), a lightweight architecture for efficient operator learning. MCNO learns the kernel of an integral operator directly and approximates it using a Monte Carlo-based approach with only a single random sample from the

grid at the start of training. By avoiding spectral transforms and deep hierarchical architectures, it offers a simple alternative that balances computational efficiency and accuracy. While our benchmarks focus on PDEs posed on regular grids with periodic or homogeneous structure, MCNO itself does not assume translation invariance or rely on global basis representations. Its reliance on pointwise sampling, rather than domain-specific structure, suggests potential adaptability to unstructured or heterogeneous settings, although such cases are not explored in this work.

We evaluate MCNO on standard one-dimensional PDEs, including the Burger’s and Korteweg–de Vries (KdV) equations. Within this setting, MCNO demonstrates competitive performance compared to established neural operator models, while maintaining architectural simplicity. We also provide a theoretical analysis showing that the Monte Carlo approximation yields a bounded bias and variance under mild regularity assumptions, and note that the result applies in arbitrary spatial dimension, suggesting the potential for broader applicability.

Contributions. The key contributions of this paper are:

- We introduce MCNO, a neural operator architecture that uses Monte Carlo-type integration with one-time random sampling to approximate solution operators for PDEs.
- We incorporate feature mixing into the Monte Carlo framework, capturing both spatial and cross-channel dependencies.
- We incorporate an interpolation mechanism to reconstruct outputs on structured grids from sampled evaluations, enabling compatibility with standard data formats.
- We provide a theoretical bias bound for the Monte Carlo approximation under regularity assumptions.
- We demonstrate the effectiveness of MCNO on PDE benchmarks, showing competitive performance.

This paper is organized as follows: Section 2 presents the basics of neural operator learning. Section 3 introduces the MC Neural Operator. Section 4 outlines the experimental setup, datasets, training procedures and a comprehensive comparison with existing methods. Finally, Section 5 concludes with a discussion of potential extensions and future directions.

II. LEARNING NEURAL OPERATORS

Neural operators are a robust framework for approximating mappings between infinite-dimensional function spaces, enabling efficient solutions to parametric partial differential equations (PDEs). This framework, originally proposed in works such as [1], [2], [8], builds upon the idea of generalizing across resolutions, making neural operators flexible and computationally efficient. Unlike traditional numerical solvers, which are often tied to specific discretizations, neural operators leverage mesh-invariant architectures to enable tasks such as optimization, inverse modeling, and real-time simulations. These properties make neural operators particularly well-suited for scenarios requiring repeated PDE evaluations, such as those encountered in engineering and scientific applications.

A. Operator Approximation

The goal of neural operators is to learn a non-linear operator $G^\dagger : A \rightarrow U$, where $A = A(D; \mathbb{R}^{d_a})$ and $U = U(D; \mathbb{R}^{d_u})$ represent Banach spaces of functions defined on a bounded domain $D \subset \mathbb{R}^d$. From a dataset of input-output pairs $\{a_j, u_j\}_{j=1}^N$, where a_j is sampled from a probability distribution μ and $u_j = G^\dagger(a_j)$, the aim is to construct an approximation:

$$G_\theta : A \rightarrow U, \quad \theta \in \Theta,$$

where Θ is a finite-dimensional parameter space. The parameters θ are optimized by minimizing a loss function that measures the discrepancy between predicted and actual outputs:

$$\min_{\theta \in \Theta} \mathbb{E}_{a \sim \mu} [C(G(a, \theta), G^\dagger(a))].$$

B. Iterative Update Framework

Neural operators are structured as iterative architectures. The input function $a \in A$ is first transformed into a higher-dimensional representation $v_0(x) = P(a(x))$ using a local map P , typically implemented as a fully connected neural network. The representation is then updated through a sequence of transformations:

$$v_{t+1}(x) := \sigma(Wv_t(x) + (\mathcal{K}(a; \phi)v_t)(x)), \quad \forall x \in D,$$

where $W : \mathbb{R}^{d_v} \rightarrow \mathbb{R}^{d_v}$ is a linear operator, σ is a non-linear activation function, and $\mathcal{K}(a; \phi)v_t$ is a kernel integral operator parameterized by ϕ . After T iterations, the final representation $v_T(x)$ is projected back to the target space U through another local map Q .

C. Kernel Integral Operator

The kernel integral operator defines the non-local updates in the iterative framework. It is expressed as:

$$(\mathcal{K}(a; \phi)v_t)(x) := \int_D \kappa_\phi(x, y, a(x), a(y))v_t(y) dy, \quad \forall x, \quad (1)$$

where $\kappa_\phi : \mathbb{R}^{2(d+d_a)} \rightarrow \mathbb{R}^{d_v \times d_v}$ is a parameterized kernel function. This formulation extends the concept of neural networks to infinite-dimensional spaces, enabling the approximation of highly non-linear operators through the composition of linear integral transformations and non-linear activation functions.

III. MC-TYPE NEURAL OPERATOR ARCHITECTURE

The MCNO architecture follows the same iterative framework described in Section 2. The input function $a(x)$ is lifted to a higher-dimensional representation $v_0(x) = P(a(x))$, which is iteratively updated using the kernel integral operator. At each step, the update is given by:

$$v_{t+1}(x) = \sigma \left(Wv_t(x) + (\hat{\mathcal{K}}_{\text{MC}}(a; \phi)v_t)(x) \right), \quad x \in D,$$

where W is a linear transformation, σ is a non-linear activation function, and $\hat{\mathcal{K}}_{\text{MC}}(a; \phi)v_t$ is the Monte Carlo-based kernel integral operator, learned by a direct representation using a weight tensor ϕ . From now on, for ease of notation, we will denote the kernel integral and its MC estimator by $\mathcal{K}_\phi v_t$ and $\hat{\mathcal{K}}_{N, \phi} v_t$ respectively. The general architecture of MCNO is illustrated in Figure 1.

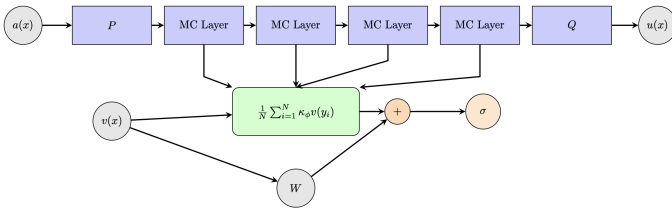


Fig. 1. MCNO's architecture

A. Monte Carlo Approximation for Integral Operators

The Monte Carlo-type Neural Operator (MCNO) uses Monte Carlo integration to approximate the integral operator defined in (1). Instead of applying deterministic quadrature or spectral transforms, MCNO estimates the operator via a simple Monte Carlo average:

$$\frac{1}{N} \sum_{i=1}^N \kappa_{\phi}(x, v_t(y_i)) v_t(y_i),$$

where $\{y_i\}_{i=1}^N$ are points sampled uniformly at random from a discretized computational grid, with sampling performed once at the start of training.

Unlike the Fourier Neural Operator (FNO), which assumes translation invariance and parameterizes the kernel in Fourier space, MCNO learns $\kappa_{\phi}(x, y)$ directly in the spatial domain without structural constraints. This enables modeling of heterogeneous or non-stationary operators. The parameters ϕ are optimized end-to-end via backpropagation.

The fixed-sample strategy avoids repeated sampling during training, supports efficient batching, and integrates with structured-grid interpolation. The method is fully differentiable and lightweight to implement.

Algorithm 1 Monte Carlo-type Neural Operator (MCNO)

- 1: **Input:** Grid points, number of samples N , kernel parameters κ_{ϕ} , and sampled points $\{y_i\}_{i=1}^N$.
- 2: **Output:** Updated representation $v_{t+1}(x)$.
- 3: Initialize the parameter ϕ .
- 4: Estimate the kernel integral $(\mathcal{K}_{\phi} v_t)(x)$ by :

$$(\hat{\mathcal{K}}_{N,\phi} v_t)(x) = \frac{1}{N} \sum_{i=1}^N \kappa_{\phi}(x, v_t(y_i)) v_t(y_i).$$

- 5: Interpolate onto the full grid
- 6: Update the representation:

$$v_{t+1}(x) = \sigma \left(W v_t(x) + (\hat{\mathcal{K}}_{N,\phi} v_t)(x) \right).$$

- 7: Optimize ϕ using the data loss function.
-

B. Efficient kernel interactions and feature mixing

MCNO leverages Einstein summation (via PyTorch's einsum operation) to efficiently compute interactions between the learnable kernel and sampled input features, i.e., $\kappa_{\phi}(x, v_t(y_i)) = \sum_j \phi_j v_{t,j}(y_i)$, where ϕ is a learnable weight tensor. This

avoids the overhead of explicit matrix multiplication and enables efficient parallelization on GPUs. Rather than aggregating over the entire grid, MCNO uses a subset of randomly sampled points to estimate the integral, maintaining efficiency while scaling to large problems.

Importantly, the learnable kernel operates over both spatial locations and feature channels. This means it not only aggregates spatial information from sampled points but also mixes input features across channels in a single operation. In contrast to models that handle spatial aggregation and channel mixing separately (e.g., with independent layers or shared weights), MCNO performs both jointly, enhancing expressiveness while keeping it computationally efficient.

C. Interpolation for grid reconstruction

Since the Monte Carlo integral is computed at a subset of sampled points, interpolation is required to reconstruct a structured grid representation compatible with standard neural architectures. In MCNO, this step maps sparse Monte Carlo estimates onto a dense discretized domain while preserving the local function structure.

MCNO employs continuous interpolation, typically using linear interpolation for smooth approximations while maintaining efficiency. However, for functions with sharp transitions, nearest-neighbor interpolation may prevent excessive smoothing. By decoupling function evaluation from grid constraints, MCNO enables flexible operator learning in both structured and irregular domains, adapting to complex spatial variations.

D. Linear Complexity

The Monte Carlo-type Neural Operator (MCNO) achieves linear computational complexity with respect to the number of samples N , offering an efficient method for approximating kernel integral operators. In contrast, the Fourier Neural Operator (FNO) computes the integral operator using the Fast Fourier Transform (FFT), which scales quasi-linearly as $\mathcal{O}(n \log n)$, where n is the number of discretization points. While efficient in practice, the FFT introduces a logarithmic overhead that can affect scalability on large grids or in high-dimensional settings.

The kernel integral in MCNO is estimated by averaging over a fixed set of N points sampled uniformly from a computational grid at the start of training. Under mild regularity assumptions on the integrand, we derive a theoretical bound on the approximation error, showing that both the bias and the variance of the estimator are controlled. Specifically, the bias decays with the resolution of the sampling grid N_{grid} , while the variance decreases with the number of samples N . This analysis confirms that MCNO maintains reliable approximation while keeping computational cost low.

E. Bounding the Monte Carlo estimation error

Consider the integral operator \mathcal{K}_{ϕ} defined as

$$(\mathcal{K}_{\phi} v_t)(x) = \int_D \kappa_{\phi}(x, y) v_t(y) dy,$$

and the Monte Carlo estimator for the kernel integral operator

$$\left(\hat{\mathcal{K}}_{N,\phi}v_t\right)(x) = \frac{1}{N} \sum_{i=1}^N \kappa_\phi(x, y_{s_i})v_t(y_{s_i}),$$

where $D \subset \mathbb{R}^d$ is a compact domain. Let $\{y_j\}_{j=1}^{N_{\text{grid}}}$ be a uniform grid discretization of D with spacing h in each dimension, such that $N_{\text{grid}} = (1/h)^d$.

Assumption III.1. To proceed we make the following assumptions:

- 1) **Uniform Boundedness:** There is $C > 0$ s.t. $\forall \phi, x, y \in D$, and v_t : $|\kappa_\phi(x, y)v_t(y)| \leq C$.
- 2) **Uniform Lipschitz Continuity in x :** There is $L_x > 0$ s.t. $\forall \phi, y \in D$, and $x, x' \in D$: $|\kappa_\phi(x, y)v_t(y) - \kappa_\phi(x', y)v_t(y)| \leq L_x \|x - x'\|$, and $L > 0$ s.t. $\forall y, z \in D$: $|\kappa_\phi(x, y)v_t(y) - \kappa_\phi(x, z)v_t(z)| \leq L \|y - z\|$.

Theorem III.2. *The Monte Carlo estimator $\hat{\mathcal{K}}_{N,\phi}v_t(x)$ approximates the integral operator $(\mathcal{K}_\phi v_t)(x)$ by averaging over N points $\{y_{s_i}\}_{i=1}^N$ sampled uniformly at random from the grid and under the assumptions III.1 we get with probability at least $1 - \delta$ the following estimation error bound*

$$\begin{aligned} & \sup_{x \in D} \left| \left(\hat{\mathcal{K}}_{N,\phi}v_t\right)(x) - (\mathcal{K}_\phi v_t)(x) \right| \\ & \leq C \cdot \frac{\sqrt{d}}{2} \cdot \text{Vol}(D) \cdot L \cdot N_{\text{grid}}^{-1/d} \\ & \quad + \frac{3}{2} C \sqrt{\frac{2(d \log N_{\text{grid}} + \log(\frac{2}{\delta}))}{N}}. \end{aligned}$$

This result ensures that the estimation error converges to zero with high probability for larger N_{grid} and N . The proof of this result is given in the appendix and relies on a bias-variance decomposition and high probability concentration inequalities.

IV. NUMERICAL EXPERIMENTS

We evaluate the Monte Carlo-type Neural Operator on two standard benchmark problems: Burgers' equation and Korteweg-de Vries (KdV) Equation. These benchmarks are widely used for testing operator learning methods due to their diversity in complexity and relevance to practical applications. To ensure fairness and consistency, we adopt the same datasets and experimental setups as described in [2].

MCNO is compared against several state-of-the-art operator learning methods and machine learning baselines. Table I provides an overview of the methods, their description, and references. The MCNO employs a four-layer architecture of Monte Carlo kernel integral operators, with ReLU activations. Training uses 1000 samples, with 100 additional samples reserved for testing. Optimization is performed with the Adam optimizer, starting at a learning rate of 0.001, halved every 100 epochs over a total of 500 epochs. We set $d_v = 64$, $N = 100$ for Burger's equation and $N = 75$ for Korteweg-de Vries (KdV) equation. All experiments are conducted on an Tesla V100-SXM2-32GB of memory GPU and the accuracy is

TABLE I
BENCHMARK MODELS EVALUATED IN COMPARISON TO MCNO.

Initials	Model Description	Reference
FNO	Fourier Neural Operator	[2]
WNO	Wavelet Neural Operator	[5]
MWT	Multiwavelet Neural Operator	[4]
MGNO	Multipole Graph Neural Operator	[9]
GNO	Graph Neural Operator	[7]
LNO	Low-Rank Neural Operator, similar to DeepONet	[1]

reported in terms of relative L_2 loss. Across both benchmarks, MCNO outperforms FNO and achieves competitive results in general, while maintaining linear computational complexity in the integration step. The errors for the main benchmarks FNO, MWT and WNO are reported with our implementation on the same GPU that we used to train our model. For the other benchmarks: GNO, LN and MGNO, the errors are taken from [4]. In this work the models were trained and tested on an Nvidia V100-32GB GPU, therefore the comparison with their reported errors is fair to a certain extent.

A. Burgers' Equation

The one-dimensional Burgers' equation is a nonlinear PDE commonly used to model viscous fluid flow. The equation is expressed as:

$$\begin{aligned} \partial_t u(x, t) + \partial_x \left(\frac{u^2(x, t)}{2} \right) &= \nu \partial_{xx} u(x, t), \\ x \in (0, 1), t \in (0, 1], \end{aligned}$$

with periodic boundary conditions and initial condition $u(x, 0) = u_0(x)$. Here, u_0 lies in $L^2_{\text{per}}((0, 1); \mathbb{R})$, and $\nu > 0$ is the viscosity coefficient.

1) *Dataset and Problem Setup:* The initial condition $u_0(x)$ is generated from a Gaussian distribution $\mu = \mathcal{N}(0, 625(-\Delta + 25I)^{-2})$, where periodic boundary conditions are applied. The equation is solved using a split-step method: the heat equation component is handled in Fourier space, while the nonlinear term is advanced using a fine forward Euler method. Solutions are computed on a high-resolution grid (8192 points) and then subsampled to lower resolutions for training and testing. The goal is to learn the operator mapping $G^\dagger : L^2_{\text{per}}((0, 1); \mathbb{R}) \rightarrow H^r_{\text{per}}((0, 1); \mathbb{R})$, defined as $u_0 \mapsto u(\cdot, 1)$ for $r > 0$.

2) *Results and Comparisons:* Table II presents benchmark results for different neural operator methods on the 1D Burgers' equation across varying resolutions. The proposed Monte Carlo Neural Operator (MCNO) achieves competitive performance, demonstrating its effectiveness in learning operator mappings. Compared to existing approaches, MCNO achieves lower error than GNO, LNO, MGNO, and FNO across all resolutions. Notably, MCNO outperforms FNO on speed and accuracy at every resolution.

The WNO seems to perform best on higher resolutions, the model is not consistent through all resolutions making it not

suitable for training on coarse grid and evaluating on finer grid. Moreover, it is slower than FNO and MCNO.

While the MWT Leg model achieves the lowest consistent error, it relies on specialized structured representations and is significantly more computationally expensive. In contrast, MCNO achieves a significant balance between accuracy, efficiency, and adaptability, offering a faster alternative to MWT Leg while maintaining competitive accuracy.

Figure 2 indicates that the relative L_2 loss is consistent with the number of samples used. As the number of samples increases the errors tend to be stable. The time per epoch is also consistent with the number of samples showing the efficiency of the MCNO as seen in Figure 3.

B. Korteweg-de Vries (KdV) Equation

The Korteweg-de Vries (KdV) equation is a one-dimensional nonlinear partial differential equation used to model shallow water waves and nonlinear dispersive phenomena. Originally introduced by Boussinesq and later rediscovered by Korteweg and de Vries, it is known for its ability to describe solutions and other complex wave interactions. Its dynamics are governed by the equation:

$$\frac{\partial u}{\partial t} = -0.5u \frac{\partial u}{\partial x} - \frac{\partial^3 u}{\partial x^3}, \quad x \in (0, 1), t \in (0, 1],$$

where $u(x, t)$ is the solution field.

1) *Dataset and Problem Setup.*: The task is to learn the mapping from the initial condition $u_0(x) = u(x, t = 0)$ to the solution at the final time $u(x, t = 1)$. The initial conditions $u_0(x)$ are sampled from Gaussian random fields with periodic boundary conditions, defined as:

$$u_0 \sim \mathcal{N}(0, 7^4(-\Delta + 7^2 I)^{-2.5}),$$

where Δ represents the Laplacian operator. The equation is numerically solved using the Chebfun package at a high resolution of 2^{10} . Notably, we utilize the same dataset as presented in [4], ensuring consistency with prior work. Lower-resolution datasets are generated by systematically sub-sampling the high-resolution solutions.

The nonlinear nature of the KdV equation and its sensitivity to the initial conditions make this a challenging benchmark for operator learning methods. Accurate solutions require capturing both the advection and dispersive behaviors of the equation.

2) *Results and Comparisons.*: Table III reports benchmark results for various neural operator models on the Korteweg–de Vries (KdV) equation at different input resolutions. Similar to the Burgers’ equation results, MCNO consistently outperforms FNO, MGNO, LNO, and GNO, demonstrating its ability to capture nonlinear dynamics effectively. While MWT Leg achieves the lowest error, MCNO remains a robust alternative, balancing accuracy and computational efficiency through its Monte Carlo-based formulation.

Figure 4 shows how the relative L_2 loss remains consistent with the number of samples. As the number of samples that are considered increases the results tend to converge. The time taken per epoch does not change much with the number of

samples showing the efficiency of the MCNO as seen in Figure 5.

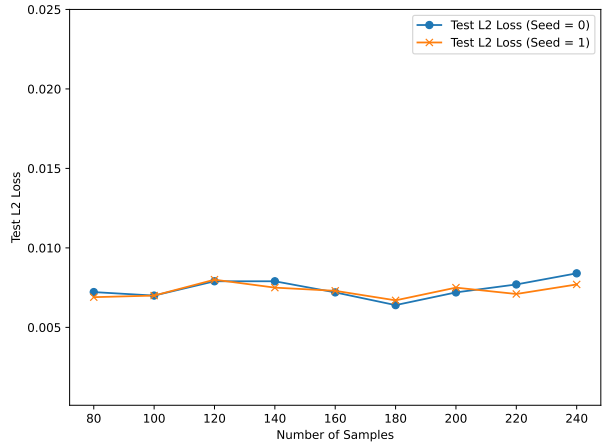


Fig. 2. L_2 test loss vs Number of samples for Burgers

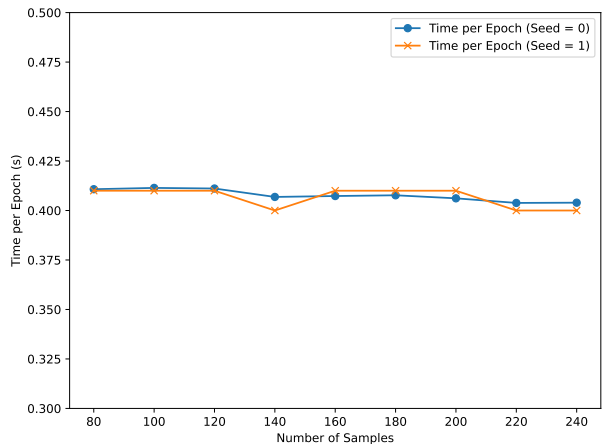


Fig. 3. Time per epoch vs Number of samples for Burgers

V. CONCLUSION

In this work, we introduced the Monte Carlo-type Neural Operator (MCNO), a lightweight operator-learning framework that directly learns kernel functions and employs a single Monte Carlo-type sampling procedure to approximate integral operators. Unlike spectral or hierarchical approaches, MCNO avoids assumptions of translation invariance and does not rely on global basis functions, enabling flexibility across grid resolutions and problem settings.

Through experiments on one-dimensional PDE benchmarks, including Burgers’ and Korteweg–de Vries (KdV) equations, we showed that MCNO achieves competitive accuracy while maintaining computational efficiency and architectural simplicity. Complementing these empirical findings, our theoretical

TABLE II
BENCHMARKS ON 1-D BURGERS' EQUATION SHOWING RELATIVE L_2 ERRORS FOR DIFFERENT INPUT RESOLUTIONS s .

Model	Time per epoch ($s=256$, $s=8192$)	$s = 256$	$s = 512$	$s = 1024$	$s = 2048$	$s = 4096$	$s = 8192$
GNO	-	0.0555	0.0594	0.0651	0.0663	0.0666	0.0699
LNO	-	0.0212	0.0221	0.0217	0.0219	0.0200	0.0189
MGNO	-	0.0243	0.0355	0.0374	0.0360	0.0364	0.0364
WNO	(2.45s, 3.1s)	0.0546	0.0213	0.0077	0.0043	0.0027	0.0012
FNO	(0.44s, 1.56s)	0.0183	0.0182	0.0180	0.0177	0.0172	0.0168
MCNO	(0.40s, 1.32s)	0.0064	0.0067	0.0062	0.0069	0.0071	0.0065
MWT Leg	(3.70s, 7.10s)	0.0027	0.0026	0.0023	0.0024	0.0025	0.0023

TABLE III
KORTEWEG-DE VRIES (KdV) EQUATION BENCHMARKS SHOWING RELATIVE L_2 ERRORS FOR DIFFERENT INPUT RESOLUTIONS s .

Model	Time per epoch ($s=128$, $s=1024$)	$s = 128$	$s = 256$	$s = 512$	$s = 1024$
MWT Leg	(3.24s, 4.96s)	0.0036	0.0042	0.0042	0.0040
MCNO	(0.36s, 0.49s)	0.0070	0.0079	0.0088	0.0081
FNO	(0.48s, 0.50s)	0.0126	0.0125	0.0122	0.0133
MGNO	-	0.1515	0.1355	0.1345	0.1363
LNO	-	0.0557	0.0414	0.0425	0.0447
GNO	-	0.0760	0.0695	0.0699	0.0721

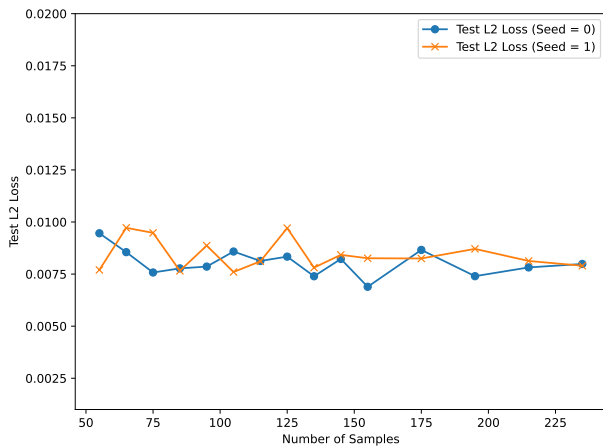


Fig. 4. L_2 test loss vs Number of samples for KdV

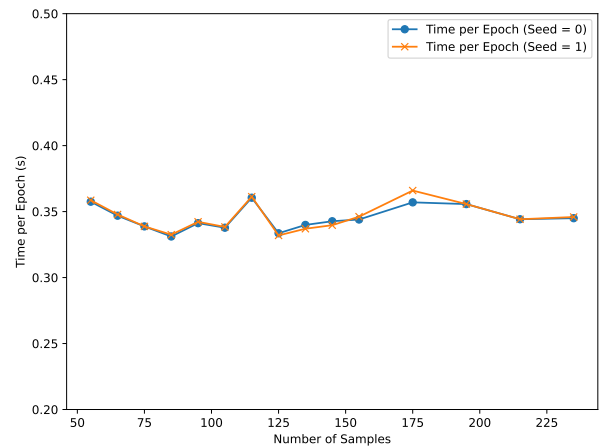


Fig. 5. Time per epoch vs Number of samples for KdV

analysis provided guarantees showing that the bias and variance of the Monte Carlo approximation are bounded, with results that extend naturally to higher spatial dimensions. Together, these results position MCNO as an alternative to established neural operator models such as Fourier- and convolution-based operators.

Looking ahead, extending MCNO to higher-dimensional PDEs and more complex systems, such as Navier–Stokes and Darcy flow, represents a natural next step. Further directions include exploring adaptive or problem-aware sampling strategies and evaluating MCNO on unstructured or heterogeneous domains. By combining theoretical guarantees with practical efficiency, MCNO contributes to the growing landscape of neural operators and highlights the promise of Monte Carlo-based approaches for scientific machine learning.

ACKNOWLEDGMENT

This work was supported by the NYUAD Center for Interacting Urban Networks (CITIES), funded by Tamkeen under the NYUAD Research Institute Award CG001. The views expressed in this article are those of the authors and do not reflect the opinions of CITIES or their funding agencies

REFERENCES

- [1] L. Lu, P. Jin, G. Pang, Z. Zhang, and G. E. Karniadakis, "Learning nonlinear operators via deepnet based on the universal approximation theorem of operators," *Nature Machine Intelligence*, vol. 3, no. 3, pp. 218–229, 2021.
- [2] Z. Li, N. Kovachki, K. Azizzadenesheli, B. Liu, K. Bhattacharya, A. Stuart, and A. Anandkumar, "Fourier neural operator for parametric partial differential equations," *International Conference on Learning Representations (ICLR)*, 2021.

- [3] P. Chauhan, S. E. Choutri, M. Ghattassi, N. Masmoudi, and S. E. Jabari, "Neural operators struggle to learn complex pdes in pedestrian mobility: Hughes model case study," *Artificial Intelligence for Transportation*, vol. 1, p. 100005, 2025. [Online]. Available: <https://www.sciencedirect.com/science/article/pii/S3050860625000055>
- [4] H. Gupta, K. Bhattacharya, and A. Anandkumar, "Multiwavelet-based operator learning for differential equations," *Proceedings of Machine Learning Research (PMLR)*, vol. 139, pp. 12 144–12 155, 2021.
- [5] T. Tripura and S. Chakraborty, "Wavelet neural operator for solving parametric partial differential equations in computational mechanics problems," *Computer Methods in Applied Mechanics and Engineering*, vol. 404, p. 115783, 2023.
- [6] B. Raonić, R. Molinaro, T. De Ryck, T. Rohner, F. Bartolucci, R. Alaifari, S. Mishra, and E. de Bézenac, "Convolutional neural operators for robust and accurate learning of pdes," in *Advances in Neural Information Processing Systems (NeurIPS)*, 2023.
- [7] Z. Li, N. Kovachki, K. Azizzadenesheli, B. Liu, K. Bhattacharya, A. Stuart, and A. Anandkumar, "Neural operator: Graph kernel network for partial differential equations," in *Proceedings of the International Conference on Learning Representations (ICLR)*, 2020. [Online]. Available: <https://openreview.net/forum?id=fg2ZFmXFO3>
- [8] N. Kovachki, Z. Li, B. Liu, K. Azizzadenesheli, K. Bhattacharya, A. Stuart, and A. Anandkumar, "Neural operator: Learning maps between function spaces with applications to partial differential equations," *Journal of Machine Learning Research*, vol. 24, no. 89, pp. 1–97, 2023. [Online]. Available: <https://jmlr.org/papers/v24/21-1524.html>
- [9] Z. Li, N. Kovachki, K. Azizzadenesheli, B. Liu, K. Bhattacharya, A. Stuart, and A. Anandkumar, "Multipole graph neural operator for parametric partial differential equations," *arXiv preprint arXiv:2009.01938*, 2020.

APPENDIX

A. Proof of Theorem III.2

Proof. We start with the bias-variance decomposition

$$\begin{aligned} \sup_{x \in D} \left| (\mathcal{K}_\phi v_t)(x) - (\hat{\mathcal{K}}_{N,\phi} v_t)(x) \right| \\ \leq \underbrace{\sup_{x \in D} \left| \mathbb{E}[(\hat{\mathcal{K}}_{N,\phi} v_t)(x)] - (\mathcal{K}_\phi v_t)(x) \right|}_{\text{Bias}} \\ + \underbrace{\sup_{x \in D} \left| (\hat{\mathcal{K}}_{N,\phi} v_t)(x) - \mathbb{E}[(\hat{\mathcal{K}}_{N,\phi} v_t)(x)] \right|}_{\text{Variance}}. \end{aligned}$$

Analysis of the Bias term: Since the points y_{s_i} are sampled uniformly from the grid, the expected value of the estimator is the Riemann sum over the entire grid

$$\mathbb{E} \left[(\hat{\mathcal{K}}_{N,\phi} v_t)(x) \right] = \frac{1}{N_{\text{grid}}} \sum_{j=1}^{N_{\text{grid}}} \kappa_\phi(x, y_j) v_t(y_j).$$

To bound the riemann sum error, we partition D into N_{grid} hypercubic cells $\{C_j\}_{j=1}^{N_{\text{grid}}}$, each with edge length h and volume h^d , centered at y_j . The integral over D is

$$\int_D \kappa_\phi(x, y) v_t(y) dy = \sum_{j=1}^{N_{\text{grid}}} \int_{C_j} \kappa_\phi(x, y) v_t(y) dy.$$

Thus, the bias term is

$$\left| \sum_{j=1}^{N_{\text{grid}}} \left(\int_{C_j} \kappa_\phi(x, y) v_t(y) dy - \kappa_\phi(x, y_j) v_t(y_j) \cdot h^d \right) \right|.$$

The Per-Cell error bound for each cell C_j is

$$\begin{aligned} \left| \int_{C_j} \kappa_\phi(x, y) v_t(y) dy - \kappa_\phi(x, y_j) v_t(y_j) \cdot h^d \right| \\ \leq \int_{C_j} |\kappa_\phi(x, y) v_t(y) - \kappa_\phi(x, y_j) v_t(y_j)| dy. \end{aligned}$$

By Lipschitz continuity of $\kappa_\phi(x, y) v_t(y)$ for fixed x and since the maximum distance from y_j to any point in C_j is $\frac{\sqrt{d}}{2}h$, thus $\int_{C_j} \|y - y_j\| dy \leq \frac{\sqrt{d}}{2}h \cdot h^d$, the per-cell error is

$$\int_{C_j} |\kappa_\phi(x, y) v_t(y) - \kappa_\phi(x, y_j) v_t(y_j)| dy \leq L \cdot \frac{\sqrt{d}}{2}h \cdot h^d.$$

Finally we obtain the total bias bound by summing over all cells and recalling that $h = N_{\text{grid}}^{-1/d}$

$$\begin{aligned} \text{Bias} &= \left| \int_D \kappa_\phi(x, y) v_t(y) dy - \frac{1}{N_{\text{grid}}} \sum_{j=1}^{N_{\text{grid}}} \kappa_\phi(x, y_j) v_t(y_j) \right| \\ &\leq \sum_{j=1}^{N_{\text{grid}}} L \cdot \frac{\sqrt{d}}{2}h \cdot h^d = \frac{\sqrt{d}}{2} \cdot \text{Vol}(D) \cdot L \cdot N_{\text{grid}}^{-1/d}. \end{aligned}$$

Bounding the Variance Term: Define the centered process

$$Z(x) = (\hat{\mathcal{K}}_{N,\phi} v_t)(x) - \mathbb{E} \left[(\hat{\mathcal{K}}_{N,\phi} v_t)(x) \right],$$

For any $x, x' \in D$ we have by Lipschitz continuity

$$|Z(x) - Z(x')| \leq \frac{1}{N} \sum_{i=1}^N L_x \|x - x'\| = L_x \|x - x'\|.$$

Thus, $Z(x)$ is Lipschitz continuous with constant L_x . To bound the supremum over a continuous domain, construct an ϵ -net $\{x_k\}_{k=1}^M$ of D , where for every $x \in D$, there exists an x_k such that $\|x - x_k\| \leq \epsilon$. Since $D \subset \mathbb{R}^d$ is compact, the minimal number of points M in the ϵ -net satisfies:

$$M \leq \left(\frac{2 \cdot \text{diam}(D)}{\epsilon} \right)^d,$$

where $\text{diam}(D) = \sup_{x, x' \in D} \|x - x'\|$ is the diameter of D . For each fixed x_k , $Z(x_k)$ is a sum of N independent random variables, each bounded by $2C$ (since $|\kappa_\phi(x_k, y_{s_i}) v_t(y_{s_i}) - \mathbb{E}[\kappa_\phi(x_k, y_s) v_t(y_s)]| \leq 2C$). Applying Hoeffding's inequality and taking a union bound

$$\mathbb{P} \left(\max_{k=1, \dots, M} |Z(x_k)| \geq t \right) \leq 2M \exp \left(-\frac{Nt^2}{2C^2} \right).$$

For any $x \in D$, choose x_k such that $\|x - x_k\| \leq \epsilon$ thus $|Z(x)| \leq |Z(x_k)| + |Z(x) - Z(x_k)| \leq |Z(x_k)| + L_x \epsilon$ and $\sup_{x \in D} |Z(x)| \leq \max_{k=1, \dots, M} |Z(x_k)| + L_x \epsilon$. Choosing $\epsilon = \frac{t}{2L_x}$, we get $\sup_{x \in D} |Z(x)| \leq \max_{k=1, \dots, M} |Z(x_k)| + \frac{t}{2}$. Set the probability of exceeding t to be at most δ with $2M \exp \left(-\frac{Nt^2}{2C^2} \right) \leq \delta$, that is

$$t \geq 2C \sqrt{\frac{2}{N} \left(d \log \left(\frac{4L_x \text{diam}(D)}{t} \right) + \log(2/\delta) \right)}.$$

Using $M \leq N_{\text{grid}}$ we get

$$t \geq 2C \sqrt{\frac{2}{N}} (d \log N_{\text{grid}} + \log(2/\delta)).$$

Thus, with probability $\geq 1 - \delta$

$$\text{Variance} \leq 3C \sqrt{\frac{2}{N}} \left(d \log N_{\text{grid}} + \log \frac{2}{\delta} \right).$$

The result is obtained by summing the upper bounds on the bias and variance. \square

B. Additional illustrations and Implementations

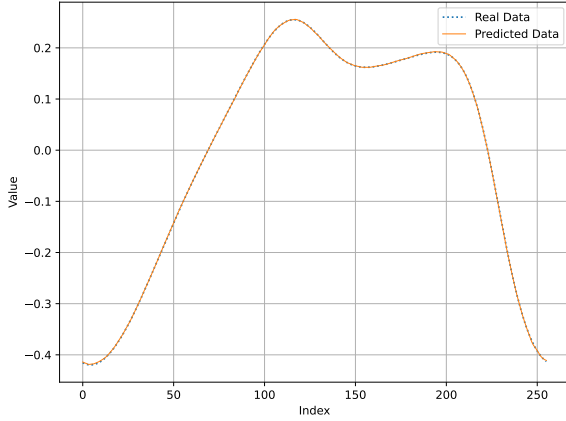


Fig. 6. Sample Prediction for Burgers

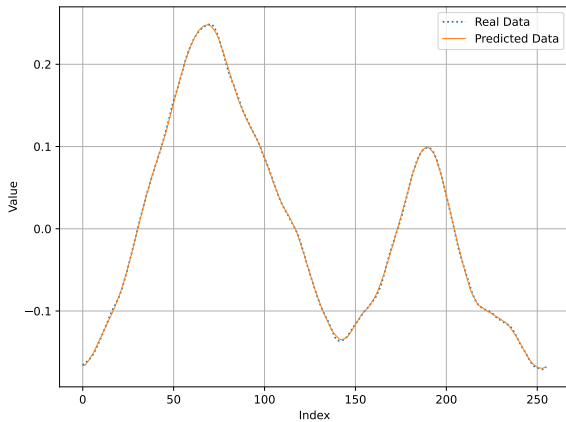


Fig. 7. Sample Prediction for KdV

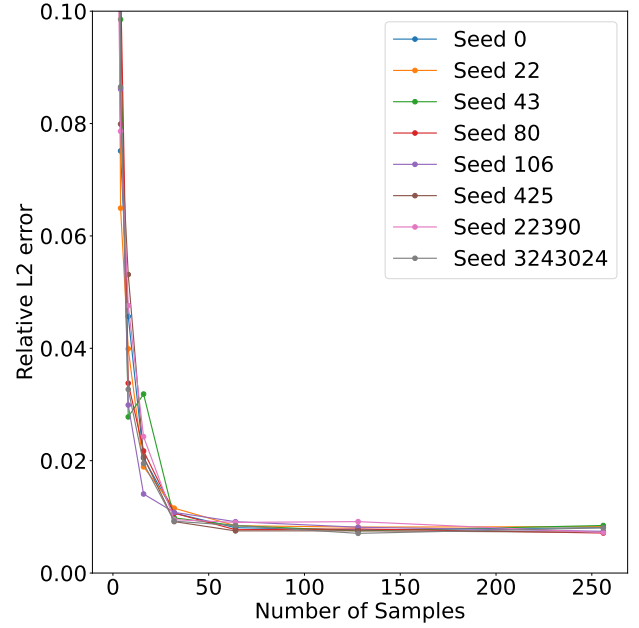


Fig. 8. Relative L_2 test loss vs Number of samples for KdV

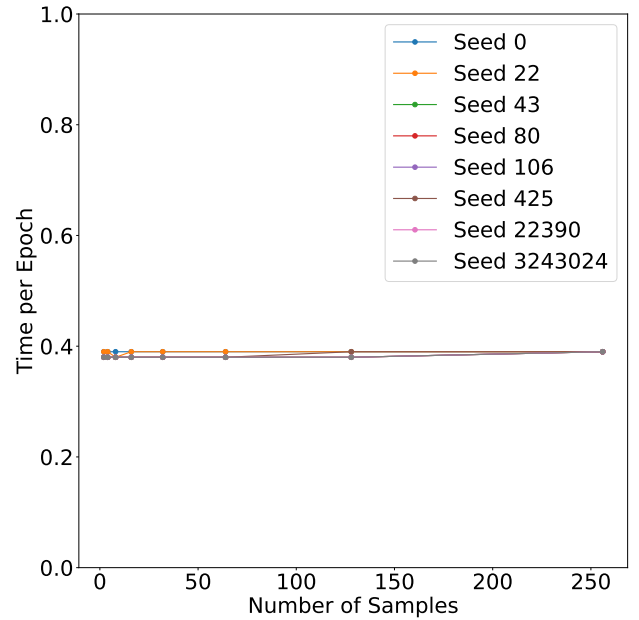


Fig. 9. Time per epoch vs Number of samples for KdV